# 4. Climatic state of the Italian Alps

V. Manara[1], A. Crespi[2], M. Maugeri[1,2], M. Brunetti[1]

*[1]CNR-ISAC, National Research Council of Italy, Institute of Atmospheric Sciences and Climate, Bologna, Italy*
*[2]University of Milano, Department of Environmental Science and Policy, Milano, Italy*

**Introduction**

The availability of an accurate description of the spatio-temporal behaviour of temperature and precipitation is becoming increasingly important and it is requested by a variety of models and decision-support tools in a wide range of fields, such as agriculture, energy production, natural resource management and preservation (Daly et al., 2002; Daly, 2006). For many applications, data at a fine (about 1 $km^2$) spatial resolution are necessary to capture environmental variability that can be partly lost at lower resolutions, particularly in mountainous and other areas with steep climate gradients. In order to provide this information for areas with complex topography, the development of suitable methodologies allowing to estimate climatological temperature and precipitation at any point of the territory and their corresponding long-term temporal evolution is needed.

Interpolation methods are highly vulnerable to fluctuations in stations' spatial coverage. This vulnerability is even more evident in mountain areas where stations are located at different elevations and absolute temperature and precipitation values present strong spatial gradients. In fact, in presence of a gap in a high elevation station the interpolated value can be biased by interpolating between adjacent valley stations. For this reason, the most widely adopted methodology to reconstruct gridded datasets is the anomaly method (New et al., 2000; Mitchell and Jones, 2005), based on the assumption that the spatio-temporal structure of the signal of a meteorological variable over a specific area can be described by the superimposition of two fields: the normals over a given reference period (i.e. the climatologies) and the departures from them (i.e. the anomalies). The formers are strongly linked to the geographical features of the territory and they can manifest remarkable spatial gradients. The most relevant aspect for their description is the availability of high-density observational dataset integrated by interpolation methods which describe the relationship between the meteorological variable and the physiographical characteristics of the Earth's surface (Daly et al., 2002, 2008; Daly, 2006). Differently, the latter are linked to climate variability and change and they are generally characterized by higher spatial coherence where the priority for their description lies in data quality and in the availability of long records.

In this context, this work describes the anomaly-based method used to reconstruct the 1951-2012 monthly temperature and precipitation records at any point of a 30-arc second resolution grid for three Italian National Parks located in the Alpine region: Gran Paradiso, Stelvio and Paneveggio - Pale di San Martino. Specifically, Section 4.1 presents the observation datasets and the methodology (local weighted linear regression - LWLR) applied to obtain the 1961-1990 temperature and precipitation climatologies for the whole Italian Alpine area. In particular, in order to assess the accuracy of the adopted method in providing the climatology over the study

area an inter-comparison with other widely used interpolation schemes is performed. Section 4.2 presents the datasets used to obtain the 1951-2012 station anomaly series (with respect to the 1961-1990 period) and the procedure adopted at first to interpolate the station series over a high-resolution grid (the same grid for which the climatologies are available) and then to superimpose them to the 1961-1990 LWLR climatologies in order to obtain a monthly absolute temperature (precipitation) records for any grid-point belonging to the three National Parks. Moreover, for each of the three areas, the mean annual and seasonal absolute series over the 1951-2012 period are presented and some episodes characterized by very low/high temperature or by intense rainfall are discussed.

## 4.1 1961-1990 high-resolution climatologies for the Italian Alps

### 4.1.1 Data

The dataset used to produce the 1961-1990 temperature and precipitation climatologies over the Italian Alpine area are recovered from many different providers at international, national, regional and local level for the Italian territory and surrounding areas (for more details see Brunetti et al. 2014 and Crespi et al. 2018 for temperature and precipitation, respectively).
All the records are subjected to quality controls by checking all sites for their position and correcting the coordinates when possible, or discarding the series if the correct location could not be identified. This step has been necessary, as incorrect elevations may induce significant errors in the estimation of the temperature/precipitation-elevation dependence. A further control on the station coordinates is also performed checking for each pair of stations if the highest correlation is associated to the closest station.
Moreover, all the monthly series are checked in order to merge series available from more than one source and, in case of overlapping time intervals, only the most reliable version is retained (usually the series with more available data).
The precipitation series are further checked by comparison with simulated series estimated from neighbouring stations. Specifically, each monthly datum in each station (test station) is estimated by means of the ten closest stations (reference stations) with an available value in correspondence with the entry under consideration ($p_{ref_i}$) and with a sufficient number of data (15 monthly values) for that month in common with the test series. Then, the test series monthly datum under consideration ($p_{test}$) is calculated as median of the single values ($\tilde{p}_{test,i}$) estimated from the ten reference series using the anomaly method:

$$\tilde{p}_{test,i} = p_{ref,i} \cdot \frac{\bar{p}_{test,i}}{\bar{p}_{ref,i}} \qquad (i = 1, \dots, 10) \qquad (1)$$

where $\bar{p}_{test,i}$and $\bar{p}_{ref,i}$ are the mean of test and reference series for the considered month over their common period.
After the quality-check, the 1961-1990 monthly temperature and precipitation normals are computed at each station site. To overcome the problem of missing data in the 1961-1990 period, the temperature normals are firstly calculated with the available data, and then re-adjusted to the

1961-1990 period by means of the Italian temperature anomaly records presented by Brunetti et al. (2006). Specifically, for each series (test series) with the 1961-1990 period partly (or fully) missing, a complete monthly local temperature anomaly (relative to the 1961-1990 period) record is calculated by a weighted average of neighbouring stations using the data and the interpolation method discussed in Brunetti et al. (2006). Then, monthly temperature normals over the same period available in the test station are calculated from this reconstructed series and subtracted to the test station normals to adjust them to the 1961-1990 interval. Moreover, all station normals are compared with those of neighbouring sites to highlight the largest discrepancies and to identify and correct possible errors. Differently, for precipitation the missing values in each station over the 1961-1990 period are estimated with the same method used for the quality-check.

For both variables the calculated normals are integrated with a small fraction of series for which the temperature and/or precipitation normals are already available (where referred to a different period they are rescaled to the 1961-1990 one).

Finally, the number of stations included in the databases and used to calculate the 30-arc-second monthly climatologies for the Italian Alpine region is 811 for temperature (Figure 1) and 2526 for precipitation (Figure 2).

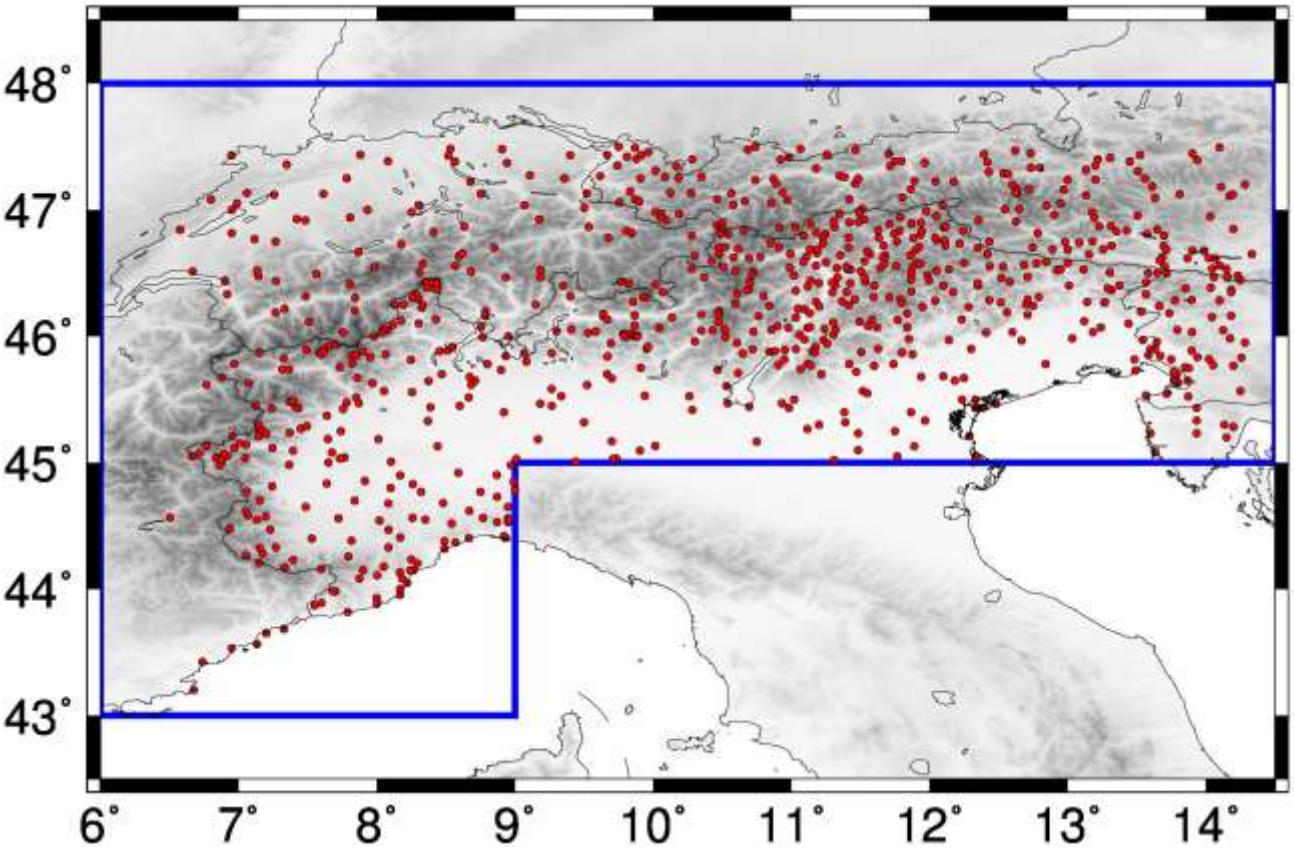


***Figure 1**. Spatial distribution of the stations included in the final database for temperature climatology reconstruction. The figure also shows the orography of the region.*

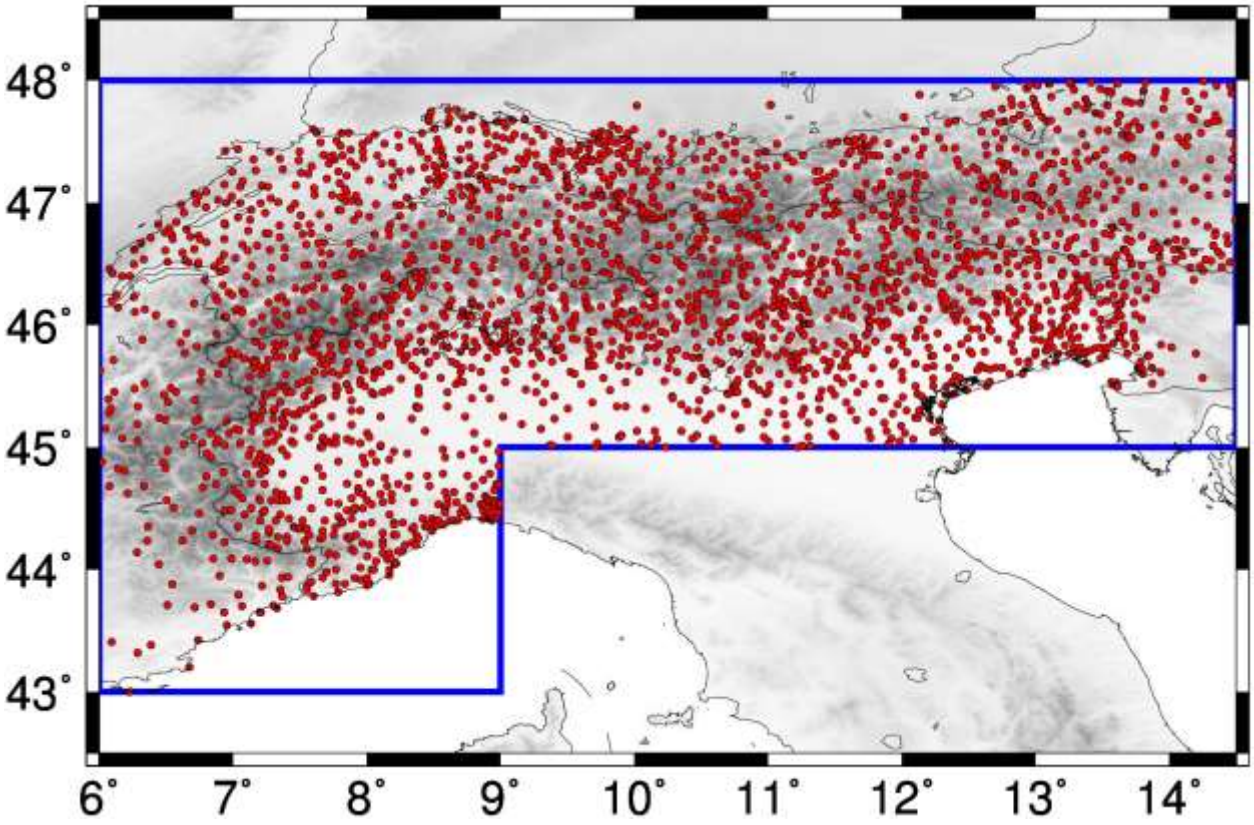


***Figure 2.*** *Spatial distribution of the stations included in the final database for precipitation climatology reconstruction. The figure also shows the orography of the region.*

#### 4.1.2 Methods

Temperature and precipitation climatologies presented in this work are computed on the 30-arc-second-resolution (about 800 m) GTOPO30 digital elevation model (DEM) (USGS, 1996) by means of a local weighted linear regression (LWLR) of temperature/precipitation *versus* elevation. This method is considered one of the most suitable approaches for areas with complex orography like the Alpine region. In order to assess its suitability, the obtained results are discussed in relation to those provided by other different methods. Specifically, for temperature the performances of a multi-linear regression with local improvements (MLRLI) (Hiebl et al., 2009) and a regression kriging (RK) (Goovaerts, 2000) are investigated too, while for precipitation a local regression kriging (LRK) and an inverse distance weighting (IDW) (Shepard, 1968) approaches are also considered.

*Local weighted linear regression (LWLR)*

The LWLR evaluates the relationship between the meteorological variable and elevation at a local level. In particular, temperature/precipitation normal $X$ at the grid-cell $(\lambda, \phi)$ is obtained as a function of its elevation $h$ by the following relation:

$$X(\lambda, \phi) = a(\lambda, \phi) + b(\lambda, \phi) \cdot h(\lambda, \phi) \qquad (2)$$

where $a(\lambda, \phi)$ and $b(\lambda, \phi)$ are the local regression coefficients.

Specifically, for any grid-cell only a cluster of stations is considered and greater weights are given to the nearest stations with topographic similarity to the target grid-cell. The stations selected for the regression (35 for temperature and 15 for precipitation) are those with the highest weights within a radius of 200 km from the given cell. More specifically, the weight of the *i*th station involved in the linear regression yielding the estimation of the climatology of the point $(\lambda, \phi)$ is the product of weighting Gaussian functions depending on position, height, distance from the sea, slope steepness and slope orientation:

$$w_i(\lambda,\phi) = w_i^r(\lambda,\phi) \cdot w_i^h(\lambda,\phi) \cdot w_i^{dsea}(\lambda,\phi) \cdot w_i^{slope}(\lambda,\phi) \cdot w_i^{facet}(\lambda,\phi) \quad (3)$$

where:

$$w_i^{var}(\lambda,\phi) = e^{-\left(\frac{\Delta_i^{var}(\lambda,\phi)^2}{c_{var}}\right)} \quad (4)$$

where *var* is the geographical feature which is being considered, $\Delta_i^{var}(\lambda,\phi)$ the absolute difference between the values of this variable at the grid-point $(\lambda,\phi)$ and that at the *i*th station location and $c_{var}$ is a coefficient which regulates the decreasing rate of the weighting and it can be expressed in terms of the value of $\Delta_i^{var}(\lambda,\phi)$ which gives a weighting factor equal to 0.5 ($\Delta_{\frac{1}{2}}^{var}$). All the details on how $\Delta_{\frac{1}{2}}^{var}$ is defined and obtained for each geographical variable are reported in Brunetti et al. (2014) for temperature and Crespi et al. (2018) for precipitation. It is important to underline that for temperature, the most appropriate $\Delta_{\frac{1}{2}}^{var}$ factors are obtained iteratively, for each month and for each geographical feature by searching for the value that gives the lowest error at station locations. Differently, for precipitation, the most appropriate $\Delta_{\frac{1}{2}}^{var}$ are locally optimised over a grid of 1°x1° resolution for each month and then interpolated onto the finest resolution grid.

An advantage of LWLR scheme is that it is possible to define a prediction interval for each grid-cell estimation. The procedure consists in estimating the variance of the temperature/precipitation of a grid-point at elevation $h_{new}$ as Daly et al. (2008):

$$s^2\{X_{h_{new}}\} = s^2\{\tilde{X}_{h_{new}}\} + MSE \quad (5)$$

where $s^2\{\tilde{X}_{h_{new}}\}$ is the variation in the possible location of the expected temperature/precipitation for a given elevation and MSE is the mean square error of the observed station temperature/precipitation values compared to those obtained by the regression model (i.e. the variation of the individual station values about the regression line). The prediction interval (with confidence α) for the grid-point with elevation $h_{new}$ is then defined as:

$$X_{h_{new}} \pm t_{\frac{1-\alpha}{2},df} \cdot s\{X_{h_{new}}\} \quad (6)$$

where *t* is the value of a Student distribution with *df* degrees of freedom (equal to the number of stations selected for the linear regression) corresponding to a cumulative probability (1-α)/2.

*Multi-linear regression of temperature with local improvements (MLRLI)*

The MLRLI approach (Hiebl et al., 2009) consists in applying, for each month, a multi-linear regression (MLR) of temperature versus elevation ($h$), longitude ($\lambda$) and latitude ($\phi$) to the entire station normal database:

$$T = m_0 + m_1 \cdot h + m_2 \cdot \lambda + m_3 \cdot \phi \qquad (7)$$

The monthly residuals from the MLR are then subjected to further analyses aiming at identifying the most significant relationships with additional physiographical variables and including in the temperature modelling the effects of sea and lake proximity, Po-Plain continentality, facet, summit/valley and urban heat islands (all details on how each term is calculated are included in Brunetti et al. (2014)). Specifically, at each step, a term is added to the MLR equation and then the monthly residuals from the new equation are considered for the evaluation of the next effect. Finally, the resulting equation is applied to each grid-cell to construct, for each month, the high-resolution temperature climatology.

*Regression kriging (RK) of temperature and local regression kriging (LRK) of precipitation*

The RK approach is applied combining to a kriging-based geostatistical approach a MLR with elevation, latitude and longitude as predictors for temperature and a local (not weighted) linear regression model with elevation as leading predictor for precipitation.
Specifically, at each grid-cell is applied Equation 7 for temperature and Equation 2 for precipitation. Here Equation 2 is applied considering all the series located within a radius optimised month by month (comprised between 125 and 200 km). The station residuals from Equation 7 and Equation 2 (ε) are interpolated on the grid by means of an ordinary kriging (OK) and added onto the regression-based fields:

$$\hat{\varepsilon}(\lambda, \phi) = \boldsymbol{k}^{\boldsymbol{T}}(\lambda, \phi) \cdot \varepsilon \qquad (8)$$

where **k** is the vector of the kriging weights for the grid-point *(λ, ϕ)*. All the details on how the RK and LRK are applied are included in Brunetti et al. (2014) for temperature and in Crespi et al. (2018) for precipitation.
It is interesting to underline that for temperature the station residuals derive from a multi-linear regression whose coefficients are estimated by using the entire station database while for precipitation the station residuals are obtained using a local approach in which the regression coefficients are defined for each grid-cell using the surrounding stations (local regression kriging – LRK).

*Inverse distance weighting (IDW) of precipitation*

The IDW approach estimates the precipitation value at an unknown point as a linear combination of a number of surrounding observations whose weights are defined by means of a Gaussian

function (Equation 4) of their distance from the target cell. Also in this method, the weighting function decay is locally optimised month-by-month following the same iterative procedure set up to estimate the best decreasing coefficients of LWLR weights.

#### 4.1.3 Performance of the interpolation models

The performances of the LWLR, MLRLI and RK for temperature and of the LWLR, LRK and IDW for precipitation are evaluated individually in terms of the ability to reconstruct the 1961-1990 observed temperature/precipitation monthly normal at station sites. Specifically, the monthly normal of all the stations contained within the study domain (607 for temperature and 1177 for precipitation – area for which the climatologies are calculated – see Figure 5 and Figure 6 for temperature and precipitation, respectively) are estimated by each model and then compared to the observed values. The reconstruction is performed in each case by means of the leave-one-out approach, i.e. by removing the station whose normal are being estimated, in order to avoid "self-influence" of the station data to reconstruct. The results of the comparison between estimated and observed values are listed in Table 1 for temperature and Table 2 for precipitation, where the monthly accuracy of each model is expressed in terms of mean error (BIAS), mean absolute error (MAE) and root mean square error (RMSE).

| | | 1 | 2 | 3 | 4 | 5 | 6 | 7 | 8 | 9 | 10 | 11 | 12 |
|---|---|---|---|---|---|---|---|---|---|---|---|---|---|
| **LWLR** | **BIAS** | 0.0 | 0.0 | 0.0 | 0.0 | 0.0 | 0.0 | 0.0 | 0.0 | 0.0 | 0.0 | 0.0 | 0.0 |
| | **MAE** | 1.0 | 0.8 | 0.7 | 0.6 | 0.6 | 0.6 | 0.6 | 0.6 | 0.6 | 0.7 | 0.8 | 1.0 |
| | **RMSE** | 1.2 | 1.1 | 0.9 | 0.8 | 0.8 | 0.8 | 0.8 | 0.8 | 0.8 | 0.9 | 1.0 | 1.2 |
| **RK** | **BIAS** | 0.0 | 0.0 | 0.0 | 0.0 | 0.0 | 0.0 | 0.0 | 0.0 | 0.0 | 0.0 | 0.0 | 0.0 |
| | **MAE** | 1.1 | 0.9 | 0.7 | 0.6 | 0.6 | 0.6 | 0.7 | 0.7 | 0.7 | 0.7 | 0.8 | 1.1 |
| | **RMSE** | 1.3 | 1.1 | 0.9 | 0.8 | 0.8 | 0.8 | 0.8 | 0.8 | 0.8 | 0.9 | 1.0 | 1.3 |
| **MLRLI** | **BIAS** | 0.1 | 0.1 | 0.1 | 0.1 | 0.1 | 0.1 | 0.0 | 0.0 | 0.1 | 0.1 | 0.1 | 0.2 |
| | **MAE** | 1.2 | 0.9 | 0.8 | 0.8 | 0.7 | 0.8 | 0.8 | 0.8 | 0.8 | 0.8 | 0.9 | 1.2 |
| | **RMSE** | 1.4 | 1.1 | 1.0 | 0.9 | 0.9 | 1.0 | 1.0 | 0.9 | 0.9 | 1.0 | 1.1 | 1.4 |

***Table 1.*** *Accuracy of the monthly temperature climatologies obtained from leave-one-out validation of the three methods (LWLR, RK and MLRLI) for the stations included in the study domain. All the values are expressed in °C. The errors are evaluated as the difference between simulated and observed values.*

| | | 1 | 2 | 3 | 4 | 5 | 6 | 7 | 8 | 9 | 10 | 11 | 12 |
|---|---|---|---|---|---|---|---|---|---|---|---|---|---|
| **LWLR** | **BIAS** | -0.1 | 0.2 | 0.3 | 0.7 | 0.8 | 0.4 | 0.1 | 0.2 | 0.1 | 0.5 | 0.5 | 0.1 |
| | **MAE** | 7.9 | 8.1 | 9.7 | 12.1 | 12.7 | 10.8 | 8.9 | 9.9 | 9.8 | 11.1 | 11.6 | 7.1 |
| | **RMSE** | 11.2 | 11.8 | 14.2 | 17.9 | 17.9 | 14.6 | 12.1 | 13.3 | 13.9 | 15.8 | 16.6 | 10.4 |
| **LRK** | **BIAS** | -0.1 | -0.1 | 0.0 | 0.0 | 0.0 | 0.0 | -0.1 | -0.1 | 0.0 | 0.1 | -0.2 | -0.2 |
| | **MAE** | 7.7 | 7.9 | 9.5 | 12.1 | 12.9 | 10.6 | 8.7 | 9.5 | 9.6 | 11.3 | 11.4 | 7.1 |
| | **RMSE** | 11.0 | 11.3 | 13.7 | 17.2 | 18.0 | 14.6 | 11.9 | 12.7 | 13.6 | 15.7 | 15.9 | 10.2 |
| **IDW** | **BIAS** | -0.1 | -0.1 | -0.2 | -0.3 | -0.4 | -0.2 | -0.1 | -0.2 | -0.2 | -0.3 | -0.3 | -0.1 |
| | **MAE** | 8.0 | 8.2 | 10.0 | 13.1 | 14.1 | 11.5 | 9.6 | 10.6 | 10.2 | 11.8 | 12.2 | 7.5 |
| | **RMSE** | 11.8 | 12.1 | 14.7 | 18.6 | 19.8 | 15.9 | 13.1 | 13.9 | 14.3 | 16.6 | 17.3 | 11.1 |

***Table 2.*** *Accuracy of the monthly precipitation climatologies obtained from leave-one-out validation of the three methods (LWLR, LRK and IDW) for the stations included in the study domain. All the values are expressed in mm. The errors are evaluated as the difference between simulated and observed values.*

The bias of LWLR and RK methods applied to temperature (Table 1) is almost null in any month suggesting that both methods are not affected by systematic errors when all the stations are considered, while MLRLI produces a small systematic positive bias indicating an overestimation of station normal (the monthly values range from 0 °C in July and August to 0.2 °C in December). The MAE and RMSE values are rather comparable for LWLR (with average equal to 0.7 °C and 0.9 °C, for MAE and RMSE respectively) and RK (with average equal to 0.8 °C and 0.9 °C, for MAE and RMSE respectively), while the highest errors are obtained for MLRLI (with average equal to 0.9 °C and 1.0 °C, for MAE and RMSE respectively).

The LWLR method applied to precipitation (Table 2) shows a small positive bias in almost all months (with average equal to 0.3 mm), while LRK and IDW show negative biases, more evident for IDW (with average equal to -0.2 mm). The MAE and RMSE show more similar values between the three methods even if LWLR (with average equal to 10.0 mm and 14.1 mm, for MAE and RMSE respectively) and LRK (with average equal to 9.9 mm and 13.8 mm, for MAE and RMSE respectively) perform better than IDW (with average equal to 10.6 mm and 14.9 mm, for MAE and RMSE respectively).

The performances of the models are further investigated by evaluating the monthly bias of appropriate station clusters. More precisely, the station bias distribution is analysed by clustering the stations within 200 m elevation belts (Figure 3 and Figure 4).

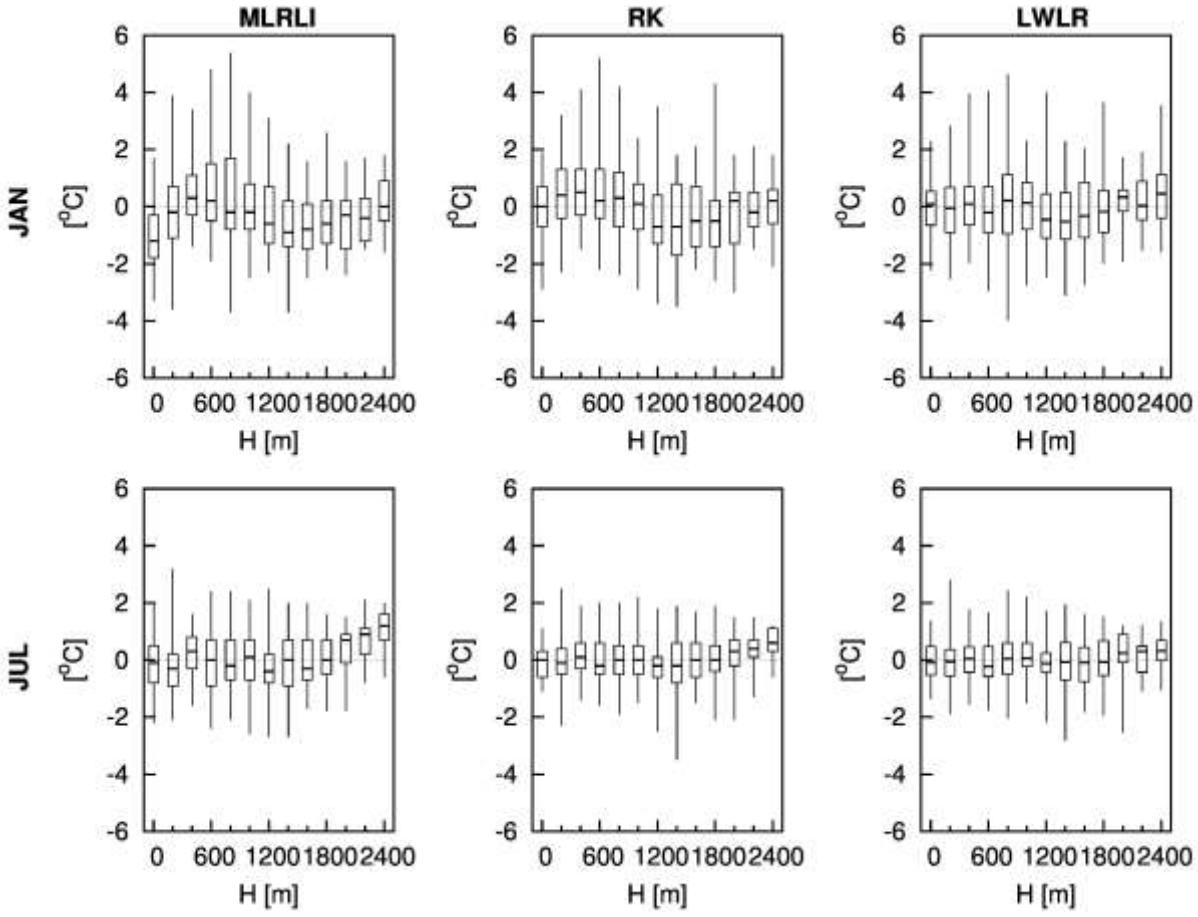


***Figure 3.*** *January (first line) and July (second line) bias (expressed in °C) distribution of the reconstructed temperature normal by the three methods (MLRLI, RK and LWLR) clustering the stations within 200 m elevation belts. Note that the last belt includes all the stations located at elevations higher than 2400 m. The boxes range from the lower to the higher quartiles and are centred on the median; the whiskers represent the minimum and maximum bias.*

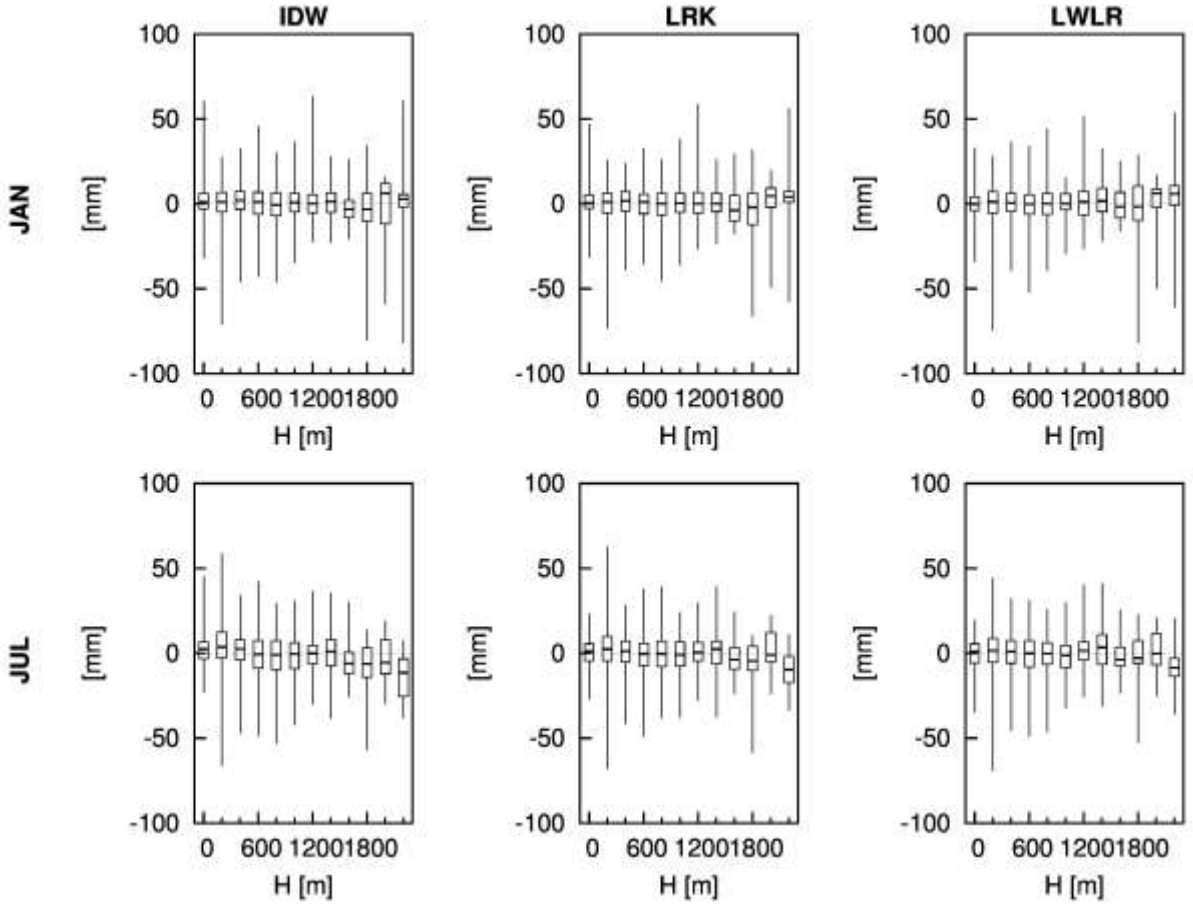


***Figure 4.*** *January (first line) and July (second line) bias (expressed in mm) distribution of the reconstructed precipitation normal by the three methods (IDW, LRK and LWLR) clustering the stations within 200 m elevation belts. Note that the last belt includes all the stations located at elevations higher than 2200 m. The boxes range from the lower to the higher quartiles and are centred on the median; the whiskers represent the minimum and maximum bias.*

As regards temperature, it is evident how the performance of the methods improves passing from MLRLI to RK and then to LWLR both in winter and in summer, especially for the highest elevations. As far as precipitation is concerned the performance improves passing from the global method (IDW) to local methods (LRK and LWLR). The results obtained for LRK and LWLR are quite comparable, but LWLR is to be preferred from the computational point of view. An advantage of LWLR method is also, as stated above, the possibility to provide, together with well performing climatology reconstructions, also an estimation of the confidence interval. For these reasons, we chose the LWLR climatologies as the definitive reconstruction to be used in the following steps for the realization of the National Parks datasets.

#### 4.1.4 High-resolution climatologies

The yearly average of the gridded monthly normals are shown for temperature and precipitation in Figure 5 and Figure 6, respectively.

A clear negative temperature gradient with increasing elevation is evident. Their annual values are comprised between -12.7°C and 15.9°C with the lowest values located in Pennine and Rhaetian Alps, while the highest values are observed in Maritime Alps. It is also worth noting the

temperature gradients occurring between the tops and the valley bottoms, especially over the Adige and Adda river basins as well as the mitigating effect of the sea.

As far as precipitation is concerned, the mean annual values range between 473 mm and 2972 mm. As for temperature, the elevation gradient is very well depicted. The highest values occur on the Carnian, Lepontine and Pennine Alps, while other very wet regions are Venetian and Orobian Alps. The driest conditions are located in the inner Alpine valleys, such as Aosta plain and the Valtellina and Adige valleys.

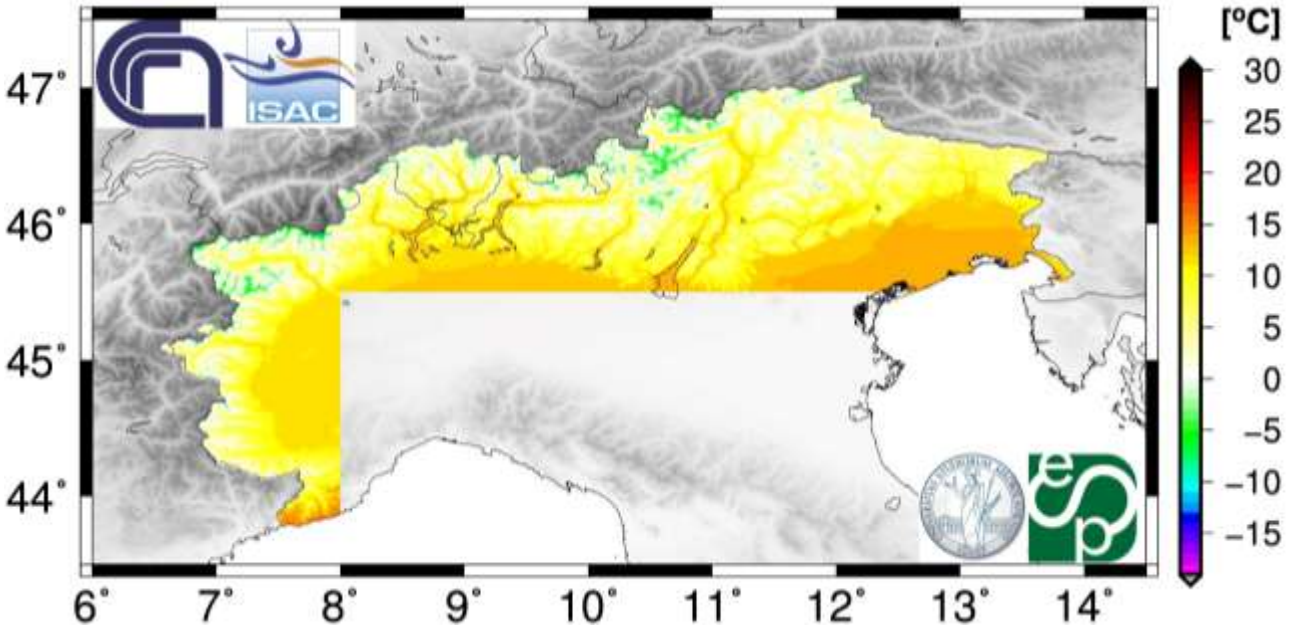


***Figure 5.*** *1961-1990 yearly temperature climatology.*

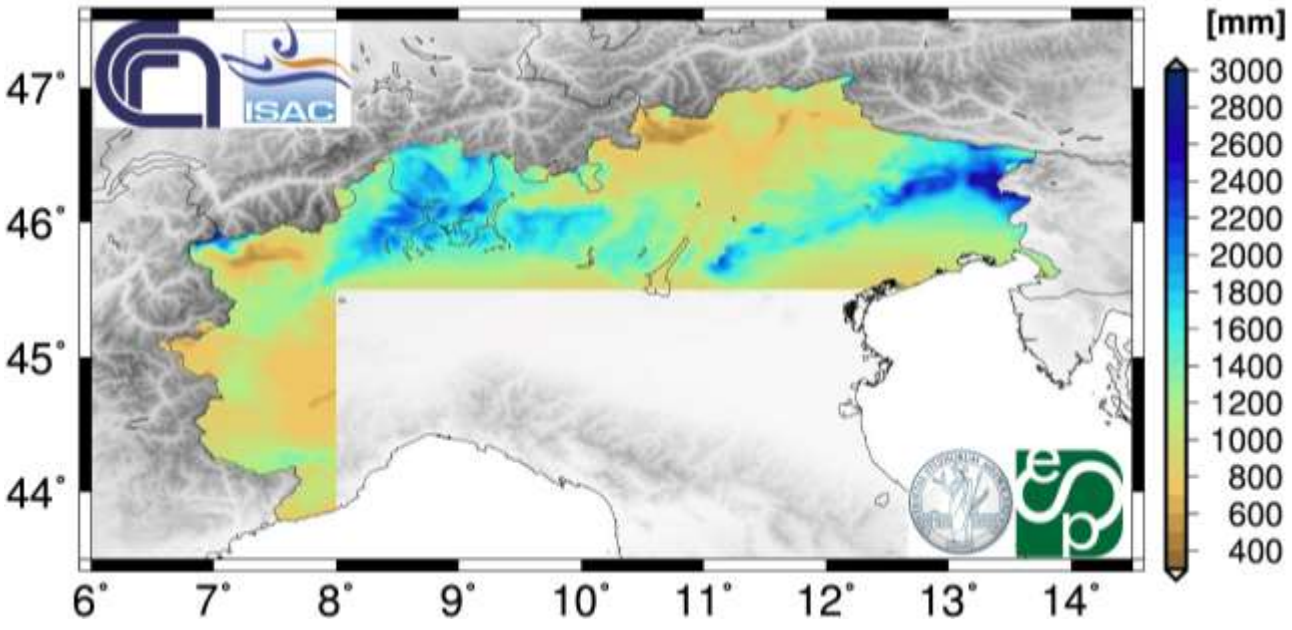


***Figure 6.*** *1961-1990 yearly precipitation climatology.*

## 4.2 Temperature and precipitation changes in three mountain National Parks (Gran Paradiso, Stelvio and Paneveggio - Pale di San Martino)

The monthly 30-arc-second-resolution temperature and precipitation climatologies for the 1961-1990 period for Gran Paradiso, Stelvio and Paneveggio - Pale di San Martino National Parks extrapolated from Figures 5 and 6 are presented in Figure 7 and Figure 8 for temperature and precipitation, respectively, together with the stations' network used for the 1951-2012 gridded temperature and precipitation temporal series reconstruction. The temperature annual values over the three parks range from -8.3°C to 11.9°C for the Gran Paradiso National Park, from -7.6°C to 10.5°C for the Stelvio National Park, and from -4.2°C to 12.2°C for the Paneveggio – Pale di San Martino National Park; while the precipitation annual values are comprised between 482 mm and 1406 mm for the Gran Paradiso National Park, between 473 mm and 1545 mm for the Stelvio National Park, and between 775 mm and 1601 mm for the Paneveggio – Pale di San Martino National Park.

### 4.2.1 Data

The databases considered for the interpolation of the 1951-2012 temperature and precipitation anomalies are independent from those used to calculate the monthly climatologies and they are collected mostly within and in the surroundings of the three boxes centred on the three parks. Specifically, they encompass 160 series for temperature (white symbols in Figure 7) with elevation comprised between 3 m (Genova Sestri) and 3580 m (Jungfraujoch) a.s.l. and 732 series for precipitation (white symbols in Figure 8) with elevation comprised between 2 m (Portesine Laguna) and 3305 m (Piz Corvatsch) a.s.l.. Before performing the interpolation, all station records are subjected to detailed quality-checks and homogenization procedures in order to remove non-climatic signals (Brunetti et al., 2006). Then, the checked station series are converted into monthly anomalies with respect to the 1961-1990 reference period (the same to which the above discussed climatologies are referred to).

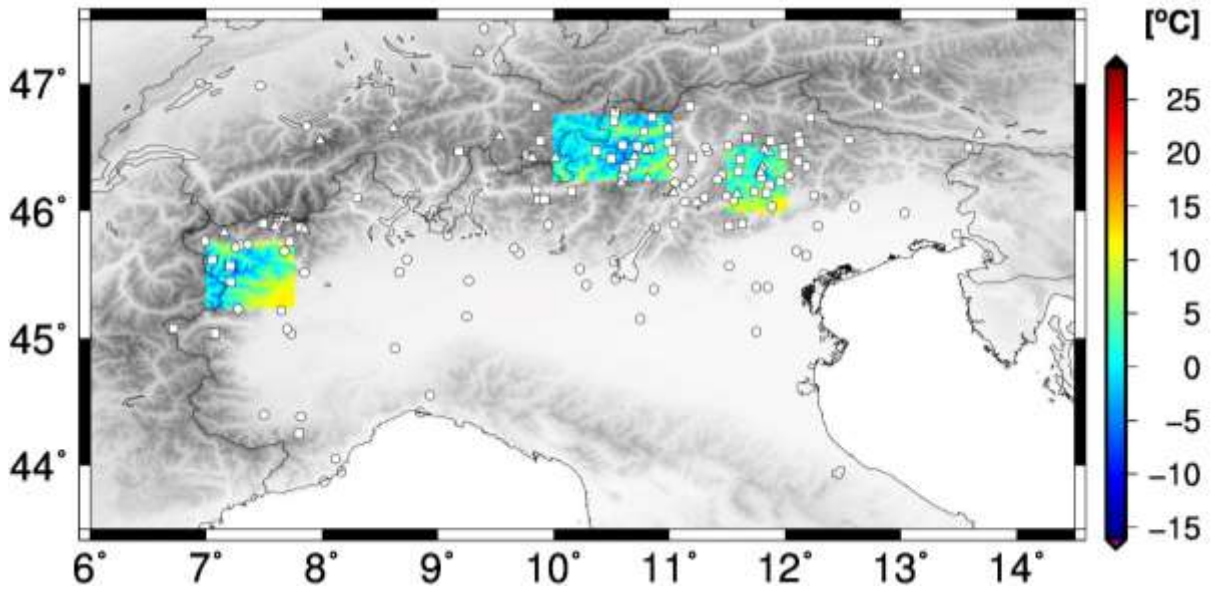


***Figure 7.*** *1961-1990 yearly LWLR (local weighted linear regression) temperature climatologies for the three analysed National Parks: Gran Paradiso (left coloured box), Stelvio (central coloured box) and Paneveggio – Pale di San Martino*

*(right coloured box). The stations considered to describe the temporal behaviour of the anomalies are represented with dots for elevations lower than 1000m, with squares for elevations higher than or equal to 1000m and lower than 2000m and triangles for elevations higher than or equal to 2000m. The figure also shows the orography of the region. The climatologies are the same of those reported in Figure 5 for the corresponding areas but they are represented with a different scale.*

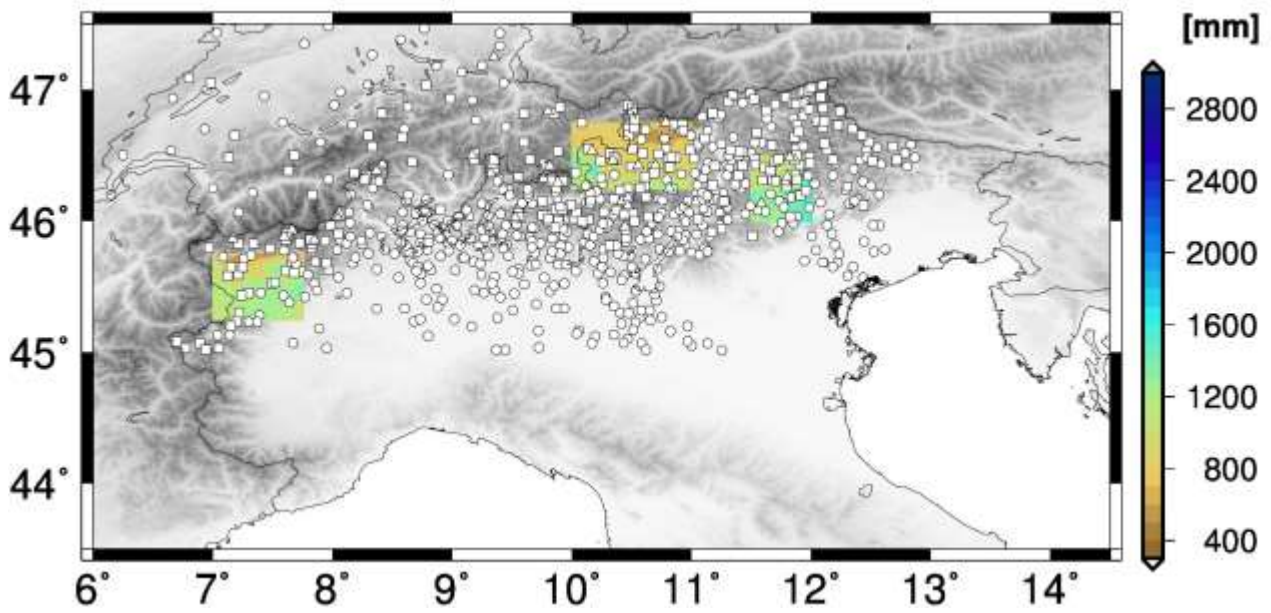


***Figure 8.*** *1961-1990 yearly LWLR (local weighted linear regression) precipitation climatologies for the three analysed National Parks: Gran Paradiso (left coloured box), Stelvio (central coloured box) and Paneveggio – Pale di San Martino (right coloured box). The stations considered to describe the temporal behaviour of the anomalies are represented with dots for elevations lower than 1000m, with squares for elevations higher than or equal to 1000m and lower than 2000m and triangles for elevations higher than or equal to 2000m. The figure also shows the orography of the region. The climatologies are the same of those reported in Figure 6 for the corresponding areas but they are represented with a different scale.*

#### 4.2.2 Methods

In order to join the information arising from the climatologies with the one of the anomalies, temperature and precipitation anomaly records are firstly interpolated from station sites onto the same high-resolution grid for which climatologies have been computed. This step is based on an improved version of the method presented by Brunetti et al. (2006). Specifically, each monthly grid-point value is calculated if there is at least 1 series at a distance lower than 50 km and 3 series at a distance lower than 100 km. The 9 stations with the highest weights are retained and their weighted mean is calculated after discarding the minimum and maximum value. If there are less than 5 available series, the weighted mean is calculated without discarding the minimum and maximum value (but this does not happen for any grid-point). The weight of each station *i* is defined by means of the product of Gaussian functions (Equation 4 in Section 4.1) depending on the distance $w_i^{rad}(\lambda,\phi)$ and elevation difference $w_i^{ele}(\lambda,\phi)$ between the i$^{th}$ station and the considered grid-point, with an additional angular weighting factor taking into account the anisotropy in the spatial distribution of the stations about the grid-point and defined as follows:

$$w_i^{ang}(\lambda,\phi) = 1 + \frac{\sum_{l=1}^{n} w_l^{rad}(\lambda,\phi)\cdot w_l^{ele}(\lambda,\phi)[1-cos\theta_{(\lambda,\phi)}(i,l)]}{\sum_{l=1}^{n} w_l^{rad}(\lambda,\phi)\cdot w_l^{ele}(\lambda,\phi)} \quad (9)$$

where $\theta_{(\lambda,\phi)}(i,l)$ is the angular separation of stations *i* and *l* with the vertex of the angle in the grid-point $(\lambda,\phi)$ and *n* is the number of stations considered to estimate the grid-point value (equal to 9 in our case). The weight halving distance (i.e., the distance for which the corresponding weight is equal to 0.5) is calculated as the mean distance from the grid-point of all stations within 100 km from it (this permits to regulate the weight decreasing rate taking into account the temporal variability in station availability), while the elevation weight halving elevation difference is set to 1000 m.

After obtaining the 1951-2012 monthly temperature and precipitation gridded anomalies, they are converted into absolute values by superimposing the corresponding 1961-1990 monthly normal. Specifically, for temperature the monthly normal are added to the monthly anomalies while for precipitation they are multiplied.

#### 4.2.3 Results

The gridded 1951-2012 seasonal (December-January-February; March-April-May; June-July-August; September-October-November) and annual temperature (precipitation) series are then averaged over each National Park domain in order to obtain a mean series representative of Gran Paradiso, Stelvio and Paneveggio - Pale di San Martino National Parks (Figure 9 and Figure 10 for temperature and precipitation, respectively). The corresponding trends are evaluated (Table 3 for temperature) by means of the Theil-Sen method (Theil 1950; Sen 1968) while the significance of the trends is evaluated by applying the Mann-Kendall non-parametric test (Sneyers 1992).

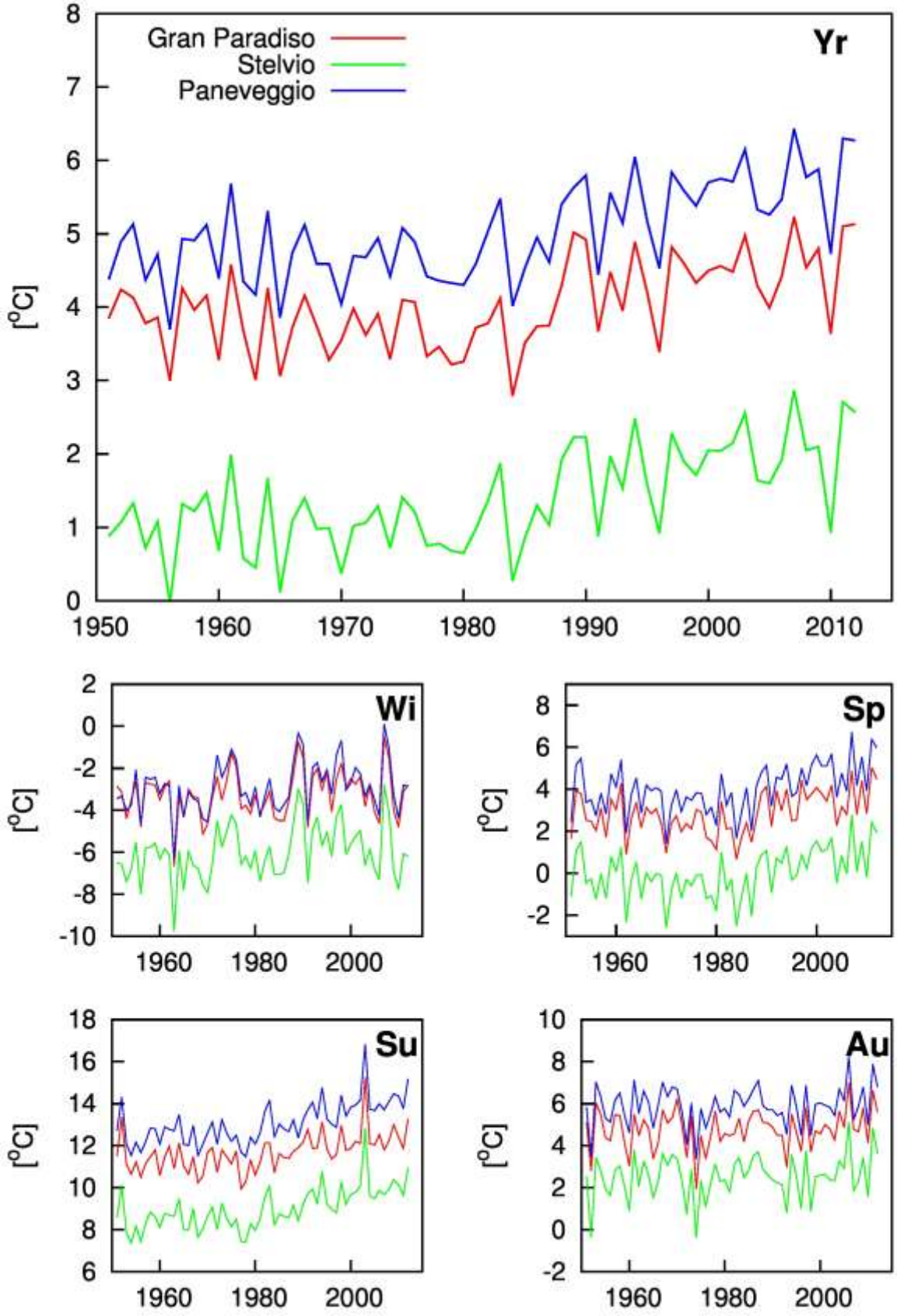


***Figure 9.*** *Absolute annual and seasonal temperature mean series for Gran Paradiso (red line), Stelvio (green line) and Paneveggio - Pale di San Martino (blue line) National Park. The series are expressed in °C.*

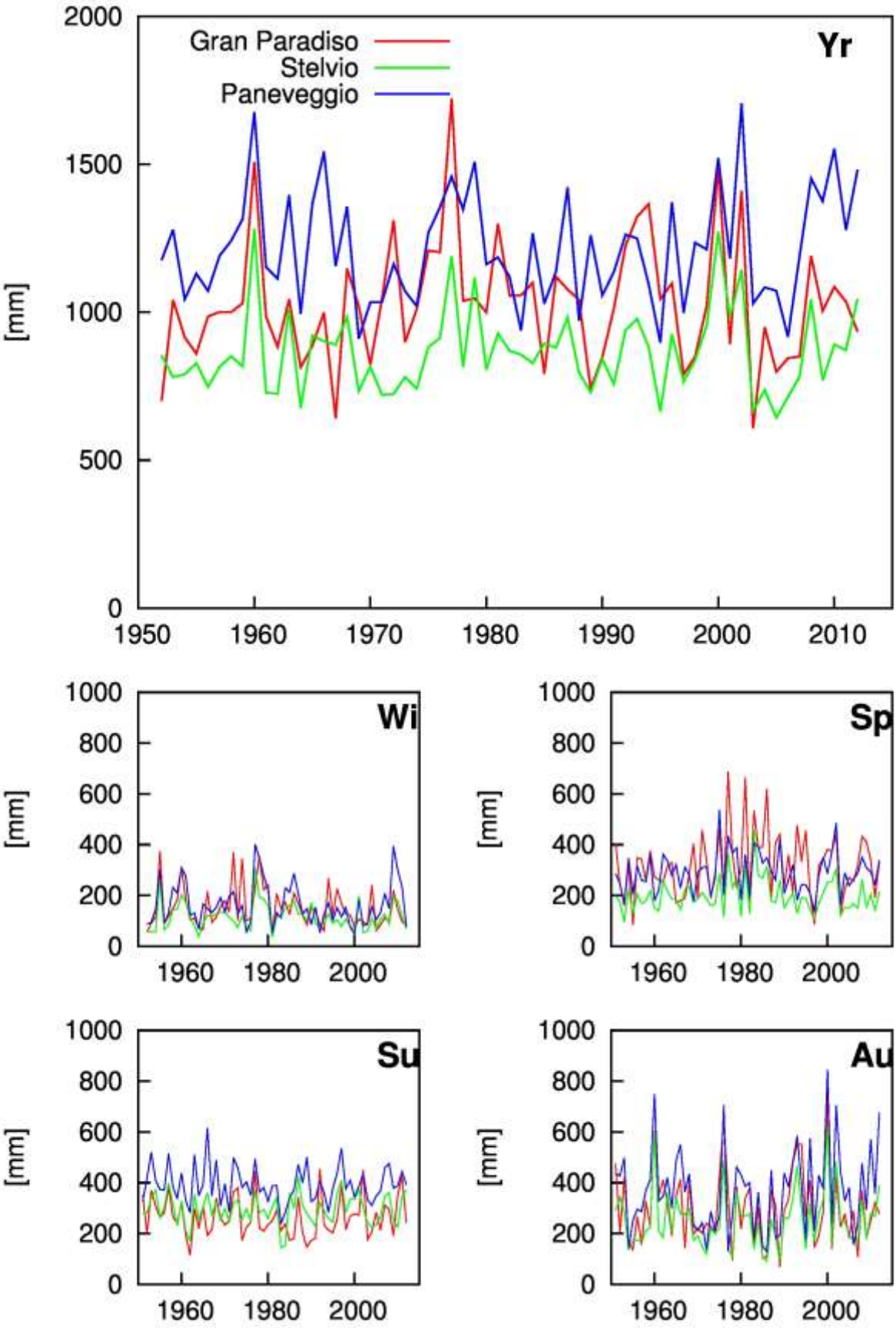


***Figure 10.*** *Absolute annual and seasonal precipitation mean series for Gran Paradiso (red line), Stelvio (green line) and Paneveggio - Pale di San Martino (blue line) National Park. The series are expressed in mm.*

| | | Winter | Spring | Summer | Autumn | Year |
|---|---|---|---|---|---|---|
| **Gran Paradiso** | **1951-2012** | + | 0.22 [0.06;0.36] | 0.24 [0.15;0.33] | + | 0.17 [0.09;0.25] |
| | **1981-2012** | + | 0.63 [0.27;1.01] | 0.32 [0.11;0.56] | + | 0.35 [0.13;0.55] |
| **Stelvio** | **1951-2012** | + | 0.28 [0.10;0.44] | 0.36 [0.26;0.45] | + | 0.24 [0.16;0.32] |
| | **1981-2012** | + | 0.70 [0.31;1.12] | 0.50 [0.27;0.74] | + | 0.38 [0.10;0.60] |
| **Paneveggio - Pale di San Martino** | **1951-2012** | + | 0.29 [0.13;0.44] | 0.36 [0.27;0.46] | + | 0.23 [0.16;032] |
| | **1981-2012** | + | 0.70 [0.33;1.09] | 0.52 [0.27;0.74] | + | 0.40 [0.18;0.59] |

***Table 3.*** *Annual and seasonal temperature Theil-Sen trends for Gran Paradiso, Stelvio and Paneveggio - Pale di San Martino National Park. Values are expressed in °C per decade and they are provided together with the lower and upper limit (in brackets – 95% confidence interval) for Mann-Kendall significance level ≤ 0.05 while for non-significant trends, only the sign of the slope is given.*

The seasonal and annual mean temperature series show a positive trend for the three areas over the whole considered period (1951-2012), significant (p-value ≤ 0.05) at annual scale and for spring and summer series. At annual scale the increase is equal to about 0.17, 0.24 and 0.23 °C per decade for Gran Paradiso, Stelvio and Paneveggio - Pale di San Martino National Parks, respectively. However, it is interesting to note that the positive trend is mainly driven by the increase starting from 1980s with values equal to about 0.35, 0.38 and 0.40 °C per decade for Gran Paradiso, Stelvio and Paneveggio – Pale di San Martino National Parks (over the 1981-2012 period) while in the previous period the temperature values do not show any trend or even a slightly decreasing tendency.

Differently, no significant trend is pointed out for precipitation on both annual and seasonal scales in all subdomains.

Besides trend analysis, the present datasets are useful for climate change impact studies. In fact, they provide a detailed information about spatial temperature and precipitation distribution over the past decades that can constitute the input for models or tools aimed to assess the effect of climate variability in a wide range of issues. As an example we present here some specific past episodes characterized by extreme temperature or precipitation events. In particular, the very low temperature of February 1956 and August 2006 and the very high values of February 1998 and August 2003 are compared in Figure 11 for the three areas.

As regards precipitation, the very intense rainfall episodes of October 2000 and November 2002, which lead to some flood events in Piedmont and Veneto, respectively, are reconstructed in Figure 12. Particularly high values are observed for Gran Paradiso during the first episode (October 2000) while high values are observed for Stelvio and Paneveggio – Pale di San Martino during the second one (November 2002).

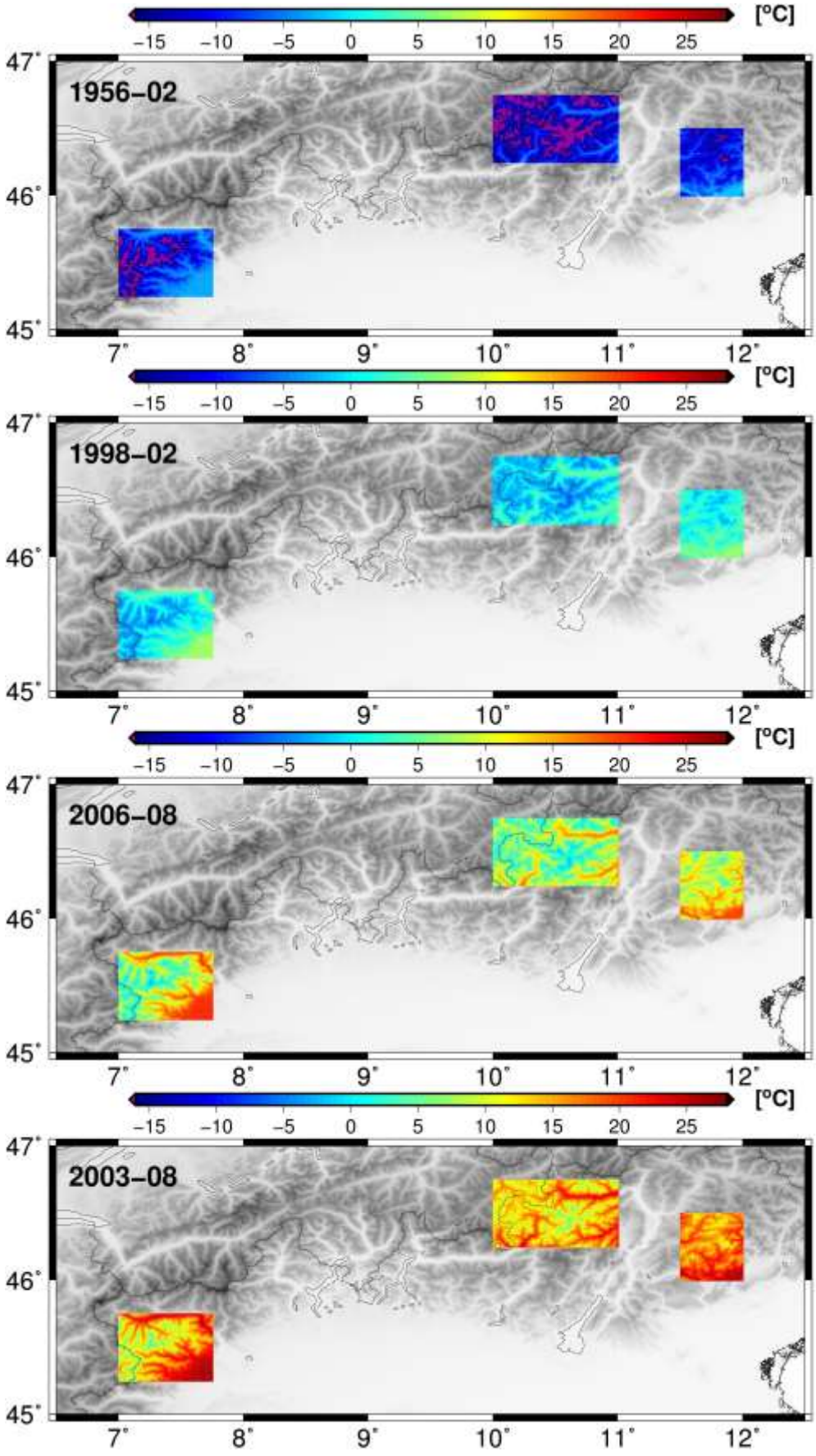


***Figure 11.*** *Temperature (expressed in °C) spatial distribution for two episodes characterized by low and high temperatures in February (first two panels) and August (last two panels) over the Gran Paradiso, Stelvio and Paneveggio - Pale di San Martino National Parks.*

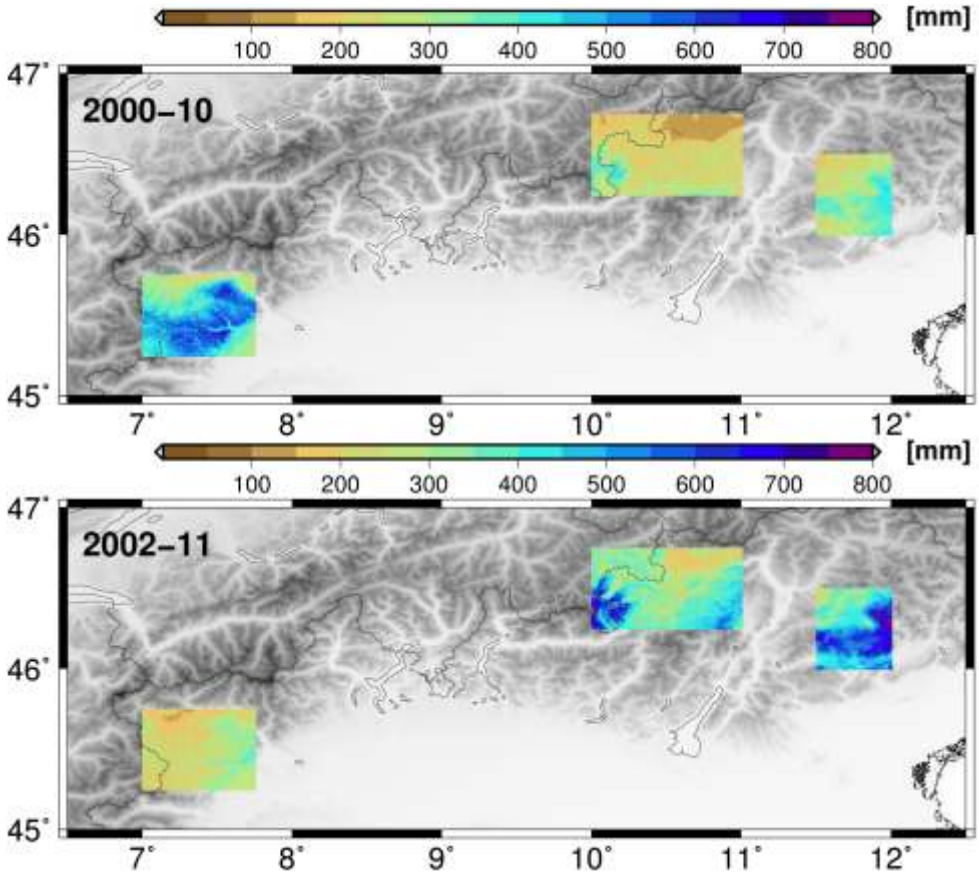


***Figure 12.*** *Precipitation (expressed in mm) spatial distribution for two episodes characterized by intense rainfall over Gran Paradiso (first panel), Stelvio and Paneveggio - Pale di San Martino (second panel) National Parks.*

**Conclusions**

The 1961-1990 monthly temperature and precipitation climatologies are reconstructed at 30 arc-second spatial resolution for the Italian Alpine region, based on dense and quality-controlled observation databases. Therefore, the anomaly-based method is applied to estimate, at the same spatial resolution, the absolute temperature and precipitation records for three National Parks located in the Italian Alpine area (Gran Paradiso, Stelvio and Paneveggio - Pale di San Martino). The series are reconstructed over the 1951-2012 period by combining the 1961-1990 normals and the gridded fields of 1951-2012 monthly anomalies.

In order to assess the performance of the adopted methodologies the resulting climatologies (estimated with a local weighted linear regression – LWLR – approach) are compared with those obtained using other methods: multi-linear regression with local improvements (MLRLI) and regression kriging (RK) for temperature and inverse distance weighting (IDW) and local regression kriging (LRK) for precipitation. The results highlighted a greater reliability of local approaches in capturing the behaviour of the meteorological variable-elevation relationship in a complex territory such as the Alpine region (Table 1 and Table 2). Moreover, it is interesting to underline that the LWLR has the advantage of providing, besides a very accurate climatology reconstruction, also the associated confidence interval. The obtained yearly LWLR temperature climatology over the Italian Alpine area (Figure 5) shows a clear temperature-elevation gradient ranging from -12.7 °C to 15.9 °C. The yearly LWLR precipitation climatology (Figure 6) shows values comprised

between 473 mm and 2972 mm with the wettest conditions in Carnia (easternmost part of the domain) and on Pennine and Lepontine Alps. On the contrary, the main inner Alpine valleys feature the driest conditions.

Then, starting from a different database, characterized by long quality-checked stations, temperature and precipitation anomaly series for the 1951-2012 period are calculated (additive anomalies for temperature and multiplicative anomalies for precipitation) and interpolated over 30-arc-second resolution grid boxes covering the three National Parks. Then, they are combined (added for temperature and multiplied for precipitation) with the 1961-1990 climatologies (Figure 7 and Figure 8) in order to obtain monthly absolute temperature and precipitation records for any grid-point belonging to the three National Parks. The temperature mean series estimated for each National Park show a positive trend over the whole considered period for all three areas, significant (p-value ≤ 0.05) for yearly (about 0.17 °C per decade for Gran Paradiso, 0.24 °C per decade for Stelvio and 0.23 °C per decade for Paneveggio – Pale di San Martino – Table 3), spring and summer series, mostly driven by the increase occurred starting from 1980s (at annual scale about 0.35 °C per decade for Gran Paradiso, 0.38 °C per decade for Stelvio and 0.40 °C per decade for Paneveggio – Pale di San Martino), while the annual and seasonal precipitation mean series do not show any significant trend in any subdomain.

The ability of the illustrated procedure is to provide an absolute temporal series of temperature and precipitation for a number of points of several orders of magnitude larger than the number of the available station records, allowing a more accurate assessment of local past variability and change useful to many climate impact related issues. Moreover, the available gridded fields can be used *i)* to extract the normals over any sub-period included in the interval spanned by the reconstructed dataset *ii)* to analyse the fine spatial structure of specific past events of extreme temperature and precipitation values and *iii)* as validation datasets to assess the reliability of the output provided by the global and regional climate models.

**References**


Brunetti M., Maugeri M., Monti F., Nanni T., 2006. Temperature and precipitation variability in Italy in the last two centuries from homogenised instrumental time series. Int. J. of Climatol., 26:345–381.

Brunetti M., Maugeri M., Nanni T., Simolo C., Spinoni J., 2014. High-resolution temperature climatology for Italy: interpolation method intercomparison. Int. J. Climatol., 34:1278–1296.

Crespi A., Brunetti M., Lentini G., Maugeri M., 2018. 1961-1990 high-resolution monthly precipitation climatologies for Italy. Int. J. Climatol., 38:878-895, doi:10.1002/joc.5217.

Daly C., 2006. Guidelines for assessing the suitability of spatial climate data sets. Int. J. Climatol., 26:707–721.

Daly C., Gibson W.P., Taylor G.H., Johnson G.L., Pasteris P., 2002. A knowledge based approach to the statistical mapping of climate. Clim. Res., 22:99–113.

Daly C., Halbleib M., Smith J.I., Gibson W.P., Doggett M.K., Taylor G.H., Curtis J., Pasteris P.A., 2008. Physiographically-sensitive mapping of temperature and precipitation across the conterminous United States. Int. J. Climatol., 28:2031–2064, https://doi.org/10.1002/joc.1688.

Goovaerts P. (2000). Geostatistical approaches for incorporating elevation into the spatial interpolation of rainfall. J. Hydrol., 228, 113–129.

Hiebl J., Auer I., Böhm R., Schöner W., Maugeri M., Lentini G., Spinoni J., Brunetti M., Nanni T., Percec Tadic M., Bihari Z., Dolinar M., Müller-Westermeier G., 2009. A high-resolution 1961–1990 monthly temperature climatology for the greater Alpine region. Meteorologische Zeitschrift 18:507–530.

Mitchell T.D., Jones P.D., 2005. An improved method of constructing a database of monthly climate observations and associated high resolution grids. International Journal of Climatology, 25:693–712, DOI: 10.1002/joc.1181.

New M., Hulme M., Jones P.D. (2000). Representing twentieth century space-time variability, Part 2: development of 1901–96 monthly grids of surface climate. J. Climate, 13:2217–2238.

Sen P.K., 1968. Estimates of the regression coefficient based on Kendall's Tau. J. Am. Stat. Assoc., 63:1379–1389, https://doi.org/10.1080/01621459.1968.10480934.

Shepard D., 1968. A two-dimensional interpolation function for irregularly-spaced data. In Proceedings of the 1968 ACM National Conference, Blue RBS, Rosenberg AM (eds). ACM Press: New York, 517–524.

Sneyers R., 1992. On the use of statistical analysis for the objective determination of climate change. Meteorol Zeitschrift, 1:247–256.

Theil H., 1950. A rank-invariant method of linear and polynomial regression Analysis. Proceedings of the Royal Academy of Sciences, 53, Part I: 386–392, Part II: 521–525, Part III: 1397–1412.

USGS (United States Geological Survey) (1996). GTOPO30 Documentation. Available at http://eros.usgs.gov/ #/Find_Data/Products_and_Data_Available/gtopo30_info.